

Morphological and Water Absorption Properties of Encapsulated Epoxy/Cellulose Nanofibrils/Nanoclay Coatings for Water Barrier and Anticorrosion Applications.

D. C. Ekweonu^{*}, I. C. Nwuzor, O. E. Ezeani, H. C. Oyeoka

Department of Polymer Engineering, Nnamdi Azikiwe University, Awka

^{*}Corresponding Author Email: cd.ekweonu@unizik.edu.ng

Abstract

The effect of water absorption properties of encapsulated nanoclay and cellulose nanofibrils on epoxy coating for barrier and anticorrosion applications was investigated. Epoxy-based nanocomposite coatings were fabricated using solution blending, with cellulose nanofibrils and nanoclay as nano-reinforcements. The nanofillers were encapsulated using the interfacial polymerization method. In this method, a polymerization reaction occurs at the interface of two immiscible phases, usually an oil phase and a water phase, to create polymeric capsules. The impact of encapsulated nanofillers on the nanocomposite coatings' water absorption and corrosion properties was investigated. The chemical constituents and nanostructure of the nanomaterials were characterized using Fourier transform infrared (FTIR) spectroscopy and transmission electron microscopy (TEM). The encapsulated nanofillers were incorporated into the epoxy-based coating and applied to steel substrates. The anticorrosion performances of the epoxy-based nanocomposite coatings were investigated through water absorption and immersion tests in NaCl solution. The TEM results demonstrate that a nanoclay of a 7 – 15 nm diameter was obtained. The water absorption study revealed that epoxy/CNF absorbed more water than epoxy/nanoclay. The sample containing 5 wt% clay and 2.5% CNF has the lowest water absorption. The water immersion test demonstrates that the plain epoxy coating, followed by the epoxy/CNF-coated metal, has greater water absorption and exhibits greater corrosion under visual inspection. The results demonstrate that the water absorption properties of epoxy-based coating can be improved by incorporating nanofillers.

Keywords: Encapsulation, Cellulose nanofibrils, Absorption, Nanocomposites, Nanoclay

1. Introduction

Polymeric coatings on metal surfaces are the most prevalent and extensively used method for preventing corrosion in metals (Mi et al., 2022; Nazari & Shi, 2016). They provide a barrier against corrosive elements such as oxygen, water, Cl⁻, H⁺ ions. They also function as a matrix to accommodate numerous corrosion inhibition species to provide active corrosion protection (Gite et al., 2015; Habib et al., 2021). It is generally known that epoxy coatings account for a significant portion of the polymeric anticorrosive coatings market because epoxy resins, a family of thermosetting polymers, have excellent performance characteristics like stability in corrosive environments and strong adhesive qualities against metallic substrates, as well as good mechanical and thermal properties (Sun et al., 2022; Wu et al., 2022). Polymeric coatings, such as polyurethane (PU), epoxy resins, and acrylics, have been broadly applied to protect metallic facilities. Research indicates that the state-of-the-art polymers alone are found insufficient in practical application for preventing the penetration of corrosive ions because the existing micro-cracks and interspaces within the polymer networks would inevitably impact their coating behavior against the corrosion medium (Li et al., 2019; Olajire, 2018). Among the various protective agents, many researchers use nanomaterials to replace the chromate-based coating immersed in aggressive media, which is mainly attributed to the enhanced anti-penetration capability of the nanocomposite (Ghazi et al., 2015).

Epoxy systems are widely used in building and civil engineering sectors due to an excellent combination of mechanical properties, chemical stability, corrosion and wear resistance, and adhesiveness to most metals and

alloys. Over the years, epoxy coatings have been widely used to protect metallic parts that are vulnerable to seawater. This is because of their innately exceptional anticorrosion and mechanical properties (Arukalam et al., 2021; Njoku et al., 2018). Furthermore, their water absorption resistance decreases due to degradation of mechanical properties by oxidation, photolysis, and ozonolysis (Zhang et al., 2017), among others. These substances from the environment produce undesirable entry points into the coatings that allow degradative organisms to enter. To reduce their susceptibility to degradation, some epoxy coatings are mixed with particulate or fibrous fillers, such as metals, metal oxides and carbonates, and clays (Dhanola et al., 2018; Matykiewicz, 2020). Among various factors to be considered for promising barrier protection, homogenous dispersion of nanofillers and their compatibility with the matrix must be ensured (Montemor, 2016). Furthermore, the corrosion inhibitors integrated corrosion mitigation coatings could form an impermeable barrier to the corrosive species and moisture, and therefore extend the life span of metallic substrates and equipment (Yang et al., 2021).

One of the methods to improve the properties of a polymeric protective coating is the addition of organic and inorganic nanofillers, leading to the formation of nanocomposite materials (Pathak et al., 2024). Nanoparticles can increase a coating's efficacy by filling in the holes and cracks in the pure polymer coating. Nevertheless, the direct application of organic and inorganic nanoparticles that inhibit corrosion into coatings may result in unfavorable interactions with the coating matrix, lowering the coating barrier qualities and inhibiting efficiency. Therefore, to maximize corrosion inhibition and prolong the active protection of polymeric coatings, encapsulation of nanoparticles (nanoclay and cellulose nanofibrils) is an effective approach to storing nanomaterials, thereby maintaining their efficiency (Gite et al., 2015). Encapsulation involves embedding nanofillers such as nanoclay (NC) and cellulose nanofibrils (CNFs) within a protective shell or matrix before incorporating them into anticorrosion coatings. This approach offers significant advantages over direct nanofiller incorporation, where nanomaterials are simply dispersed into the bulk matrix. By encapsulating nanofillers, it is possible to enhance their dispersion, improve interfacial adhesion, ensure controlled release, and maintain their functional integrity and resistance to chemical degradation—all of which are essential for achieving durable, high-performance anticorrosion coatings. These benefits often surpass those of direct nanofiller incorporation, which may lead to issues like poor dispersion, interfacial incompatibility, and uncontrolled release of the nanofillers (Kumar & Thakur, 2024; Xu et al., 2024).

Consequently, some works of literature have reported the successful application of some plant extracts (Manickam et al., 2016) as fillers in formulating water barriers, self-healing, and anticorrosive epoxy nanocomposite coatings. Some of these natural fillers (cellulose nanofibrils and nanoclay) are polymeric and have become attractive because they are cheap, non-toxic, biocompatible, biodegradable, and can easily be sourced from renewable agricultural resources. Despite the recorded successes, the durability of some of these plant extracts for water barrier, anticorrosion, and self-healing applications has remained a great source of worry (Ramesan & Surya, 2016). Cellulose nanofibrils (CNFs) have been used for a variety of major applications in the field of materials science, mainly due to their high mechanical properties, smaller dimensions, high surface-to-volume ratio, renewability, and biodegradability (Ewulonu et al., 2020; Velásquez-Cock et al., 2016). Cellulose fibrils with lengths and widths in the micro- and nanoscales, either individually or in groups. CNF is also a potent gas barrier substance. The oxygen permeability of CNF films can be well compared with some of the commercially available petroleum-based polymers under low-humidity conditions (Nair et al., 2017). In the context of developing a suitable green filler for epoxy resin coatings, the coupling of cellulose nanofibers with nanoclay (kaolinite) is proposed (Surendran et al., 2021).

Over the past two decades, researchers have increasingly incorporated nanoclay into epoxy resins and other polymers because of their special properties. These special properties (improved barrier properties, increased mechanical strength, enhanced thermal stability, improved flame retardancy, better adhesion and scratch resistance, reduced shrinkage and curing stress, and enhanced chemical resistance) come from the unique layered structure and high surface area of clays, particularly when they are well-dispersed in the resin. Blending epoxy resins and small quantities of nanoclays on a molecular level greatly improved the mechanical, thermal, and especially barrier and anticorrosive performances compared to the neat epoxy resins (Iheoma & Isaac, 2016; Motlatle et al., 2018). In this study, the CNF and nanoclay (kaolinite clay mineral) were encapsulated and used to reinforce epoxy coatings. The interfacial polymerization method was used to prepare the nanocapsules. Incorporating CNF/NC capsules to enhance the properties of widely accepted polymeric coatings, like epoxy coatings, has yet to be reported in the literature. Therefore, this study aims to produce a nanocomposite coating using encapsulated nanoreinforcements for enhanced water barrier and corrosion protection in a saline environment.

2.0 Materials and methods

2.1 Materials

The cellulose nanofibrils used in this study were obtained from a previous work by Ewulonu et al. (2020). The study reported the CNF particles' size ranging between 1 and 19 nm, with several micrometers apart. The local clays used in this study were sourced from two different locations, Nsu in Ehime Mbanjo Local Government Area and Etiti in Ihitte-Uboma Local Government Area within the South-Eastern region of Nigeria. Initial preparations of the clays were done as stated by Chukwujike and Igwe, 2016. Cellulose nanofibrils and nanoclay served as the primary components. A solution of urea and formaldehyde (37 wt% formaldehyde in water) was utilized to synthesize the polyurea formaldehyde (PUF) shell. Deionized (DI) water was used to cleanse the nanocapsules. Sodium dodecylbenzene sulfonate (SDBS) served as the surfactant, while poly(vinyl alcohol) (PVA) functioned as the stabilizer. Resorcinol served as the crosslinker, whereas ammonium chloride functioned as the co-reactant in synthesizing capsules. Sodium hydroxide (NaOH) and sulphuric acid (98 %) were employed to regulate the pH of the system. Bisphenol A epoxy served as the coating resin, while polyamide functioned as the curing agent. Xylene served as the solvent in the coating composition. Steel served as the substrate, while sodium chloride (NaCl) was utilized to prepare simulated seawater (corrodent). All other reagents and chemicals were of analytical grade and used as obtained from the Onitsha Head-Bridge chemical market, Anambra State.

2.2 Nanoclay Preparation

The kaolin clay materials prepared from the previous work by Iheoma and Isaac (2016) were synthesized into nanoclay according to the method described by (Calabi-Floody et al., 2011). In this method, 15 g of the clay was dispersed in 300 mL of 1.5 M NaCl and centrifuged for 50 minutes at room temperature at 4000 rpm. The supernatant was decanted to eliminate mineral impurities in the first step, the average particle diameter was less than 100 nm. The sedimented fraction was accumulated throughout the centrifugation procedure and was centrifuged at 4000 rpm after being dispersed in 50 mL of distilled water with moderate agitation for 40 minutes. The supernatant was collected, while the residue was redispersed and centrifuged. This method was repeated 6 times while the supernatant containing the nanoclay was purified using distilled water. The solid nanoclay was produced by lyophilizing the refined substance.

2.3 Preparation of urea formaldehyde (UF) pre-polymer

The capsules were prepared by the interfacial polymerization method, similar to the method described by (Njoku et al., 2018). Following an established methodology, 10 g of urea and 40 ml of formaldehyde were combined in a 500 ml beaker, and the mixture was agitated at 300 rpm until a clear solution was achieved. This produced the pre-polymer, urea-formaldehyde (UF). Using NaOH, the solution's pH was brought down to 8.3. A thermostatic water bath was used to heat the mixture to 70 °C for one hour. The urea formaldehyde (UF) pre-polymer created by this technique was utilized in the encapsulating procedure.

2.4 Capsule formation

The pre-polymer was then dissolved in de-ionized water in a 1000 ml reaction beaker with 1 g PVA and 0.2 g Sodium dodecylbenzene sulfonate (SDBS). To enable the integration of nanoparticles into the pre-polymer, a suitable quantity of cellulose nanofibrils and nano-clay was added to the reaction media and aggressively agitated for 20 minutes at 500 rpm using a mechanical stirrer. Subsequently, 1 g of ammonium chloride and 1 g of resorcinol were added. The mixture was then put in a thermostatic water bath equilibrated at 70 °C for three hours. thereafter, a few drops of acid catalyst (0.5 M H₂SO₄) were added to the mixture to bring the pH down to 2.5.

The nanomaterials were encapsulated by the pre-polymer particles following a polymerization reaction that took place at the interfaces of these droplets. After retrieving the beakers holding the capsules, they were left to cool for four hours at room temperature. Filter paper and a funnel were used in the filtration process to separate the capsules from the aqueous phase. After cleaning with distilled water, the resulting capsules were allowed to air dry for a week before oven-drying for 6 hours at 50 °C. The prepared nanoclays were then carefully crushed in a mortar and sieved to nanosizes using a mesh with a pore size of 45 microns to obtain uniform particle sizes suitable for further application.

2.5 Coating Preparation

The coatings were prepared by the solution blending method, similar to the method described by Njoku et al. (2018) Two procedures were used to introduce the nano-capsules into the epoxy resin. The first phase was employed using a water bath ultrasonicator to completely dissolve a predefined weight of each of the cellulose nanofibrils and

nanoclay capsules (per the design) in 15 ml of xylem while stirring constantly for 30 minutes. Following the dispersion procedure, the nano-capsules were combined with the curing agent (polyamide) and epoxy resin (epoxy) in a 3:2 by weight ratio using a three-blade mechanical stirrer for 40 minutes. A small quantity of the epoxy nanomaterial was poured into a petri dish and allowed to air dry for five days to guarantee adequate post-drying. After peeling the coatings off the dish, they were kept in a desiccator for further evaluation.

Table 1: Formulation Table for Nanoclay-Cellulose Nanofibrils Reinforced Epoxy Coating

Sample Code	Epoxy (wt%)	NC (wt%)	CNF (wt%)	Total (wt%)
EP	100	0	0	100
EP-C2.5	97.5	2.5	0	100
EP-C5	95	5	0	100
EP-NF2.5	97.5	0	2.5	100
EP-NF5	95	0	5	100
EP-C2.5NF2.5	95	2.5	2.5	100
EP-C5NF2.5	92.5	5	2.5	100
EP-C2.5NF5	92.5	2.5	5	100
EP-C5NF5	90	5	5	100

EP=Epoxy, C=Nanoclay, NF=Cellulose nanofibrils

2.6. Fourier Transform Infrared (FTIR) Spectra

FTIR spectroscopy was conducted on the encapsulated Nanoclay (NC) and Cellulose nanofibrils (CNF) using an Equinox 55 FTIR spectrometer fitted with a golden gate single attenuated total reflection (ATR) cell to determine the presence of the encapsulated NC and CNF functional group. The transmittance mode was used to capture the FTIR spectra, which had a resolution of 4 cm⁻¹ and ranged from 4000 to 400 cm⁻¹.

2.7 Transmission Electron Microscopy (TEM)

The morphology and size distribution of the nanocomposite (NC) were examined using a JEM-2100 transmission electron microscope (TEM) operated at 80 kV. TEM analysis was also employed to assess the degree of dispersion, specifically intercalation or exfoliation, of the clay nanoplatelets within the epoxy matrix. For sample preparation, the NC was dissolved in acetone and sonicated for approximately 25 minutes to ensure uniform dispersion. A drop of the resulting colloidal suspension was deposited onto a copper grid and allowed to dry completely at room temperature. TEM images were then captured and analyzed using ImageJ 1.52 software to estimate the sizes of individual nanoparticles and determine the overall particle size distribution.

2.8 Water absorption

A water absorption test was conducted on coated samples measuring 20 x 20 x 0.2 mm to investigate the amount of water absorbed at the designated time intervals. These samples were weighed before they were submerged in 100 mL of water and observed periodically for 7 days. The test was conducted with saline water, and the electronic balance was used to measure the water absorption by deducting the sample's weight after immersion from its weight before immersion. The water absorption properties of the specimens were calculated according to Eq. 1

$$\% \text{ Water absorption} = \frac{W_t - W_i}{W_i} \times 100 \quad (1)$$

Where W_i and W_t are the initial and final weights of the sample at time t .

2.9 Immersion Test

The anticorrosive performance of the nanocomposite coatings was evaluated using the ASTM G31 standard. Metal samples coated with the nanocomposite were immersed in a 3.5 wt.% NaCl solution for 7 days. Their weights were recorded before and after immersion to calculate weight loss. Corrosion resistance was assessed based on visual inspection and the amount of weight lost during the test.

3.0 Results and Discussion

3.1 FTIR Analysis of the Nanofillers

Figure 1 represents the FTIR spectra of Nanoclay. The FTIR of the NC reveals the functional groups present in the samples. These spectra illustrate the effects of chemical and acid modifications on the nanoparticles. In both spectra, a broad absorption band observed at 4189.0 cm⁻¹ and 3683.7 cm⁻¹ corresponds to the presence of hydroxyl groups,

indicating characteristic O–H stretching vibrations. A bending vibration occurred at 4189.0 cm^{-1} , which corresponds to an O–H from phenolic groups. Also, weak bending vibrations at 3942.5 and 3883.7 cm^{-1} correspond to H and OH groups in urea and H_2SO_4 , respectively. The stretching vibration at 3642.74 cm^{-1} is the O–H stretching from free hydroxyl (not bonded to H) that may be from AL-OH or SI-OH, which are present in the Nanoclay. Such a free OH group may also come from glycerol. The peak at 3446.33 cm^{-1} is an OH group that is bonded to hydrogen. This can be found in the phenolic group, or H_2SO_4 . C–H group present in toluene and glycerol was identified at a bending peak of 2970.24 and 2930 cm^{-1} . The broad peak at 1435 cm^{-1} corresponds to (–H in toluene and N–H I urea). The peak at 874.15 corresponds to Si–O–Si in nanoclay (Saucedo-Zuñiga et al., 2021).

Figure 2 represents the FTIR spectra of Cellulose Nanofibrils. From the FTIR of the (CNFs) sample, the identified functional group is a weak bending vibration which occurred at 3750 and 3683.7 cm^{-1} , corresponding to N–H and OH groups in urea and H_2SO_4 , respectively. Also, the broad absorption band around 3400 cm^{-1} is due to the O–H stretching vibration. This result is in correlation with the study by (Cichosz and Masek, 2020), which indicates hydrogen bonding and the hydrophilic nature of CNFs. Such a free OH group may also come from resorcinol. The absorption band around 2800 cm^{-1} is attributed to C–H stretching vibrations of the glucose units (Kozłowicz et al., 2020). The bands around 1493 cm^{-1} correspond to bending vibrations of C–H bonds in cellulose (Dassanayake et al., 2023). The absorption bands around 1099 cm^{-1} are due to C–O–C stretching vibrations in glucosidic bonds linking glucose units and C–O stretching in primary and secondary alcohol groups of CNFs (Oghenekohwo, 2023). The peak at 611 cm^{-1} is associated with O–H out-of-plane bending vibration due to the hydrogen bonding network (Shao et al., 2023).

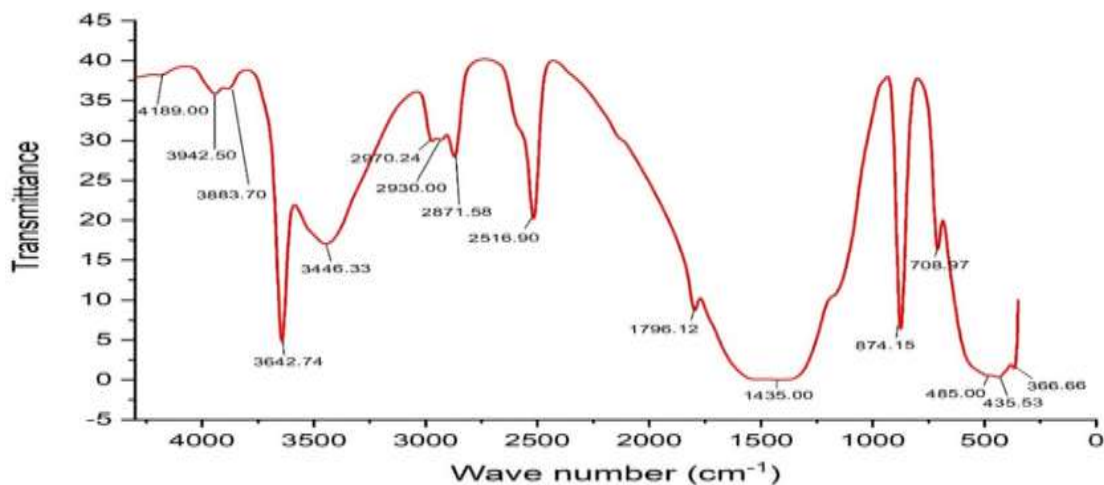


Figure 1. FTIR Spectroscopy of the nanoclay (NC) sample

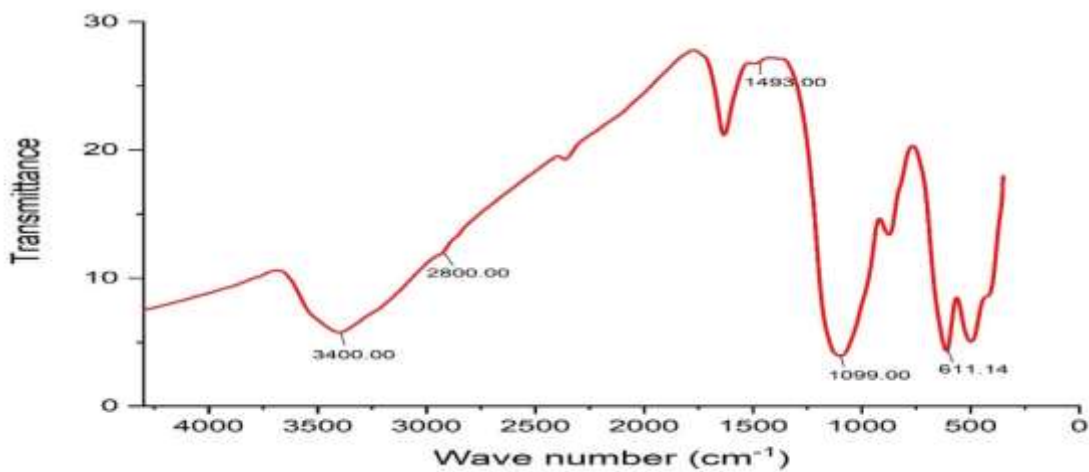


Figure 2. FTIR Spectroscopy of the Cellulose nanofibrils (CNFs) sample

3.2 TEM Analysis of Nanoclay (NC)

The TEM micrograph in Fig. 3 demonstrated that the scattered particles are spherical but varied in size, with diameters ranging from 7-15nm, which may be because of variations in the creation time of the nanoparticles. Proper functionalization of nanoparticles can create a suitable mixture and lessen agglomeration by strengthening the interphase between distinct components. The image from the figure shows a formation of exfoliated structure, well-separated and randomly dispersed clay nanoparticles in a spherical shape. A similar result was obtained by Hakamy et al. (2015) in their studies of the particle size of nanoclay, using high-resolution transmission electron microscopy (HRTEM), in their results, they observed small clay nanoparticles with approximate spherical shapes ranging 3-8 nm.

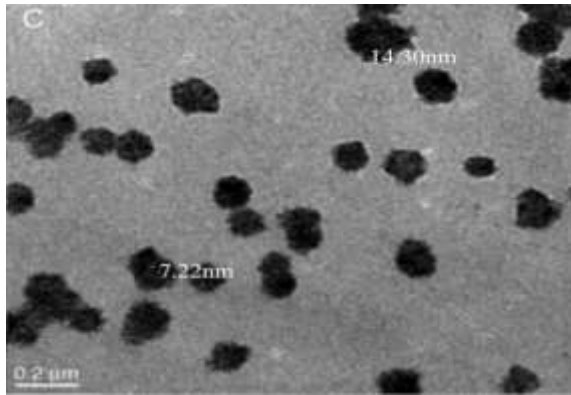


Figure 3. TEM Micrograph of the Nanoclay (NC) sample

Sample Code	Water Absorption (%)	Saline Absorption (%)
EP	1.85	1.54
EP-C2.5	1.65	1.35
EP-C5	1.45	1.20
EP-NF2.5	1.95	1.75
EP-NF5	2.25	1.85
EP-C2.5NF2.5	1.75	1.45
EP-C5NF2.5	1.60	1.30
EP-C2.5NF5	1.90	1.50
EP-C5NF5	1.70	1.40

Table 2: Water Absorption (%) for each Sample

3.3 Water Absorption

The water absorption test was conducted to evaluate the resistance of different epoxy-based coatings to water absorption. This is a key factor in the performance and longevity of protective coatings used in humid environments. Figure 4 depicts the water absorption percentages of various coating formulations, including plain epoxy (EP), epoxy with nanoclay (EP-C), epoxy with cellulose nanofibrils (EP-NF), and hybrid systems containing both nanoclay and cellulose nanofibrils (EP-C-NF). From the figure, it is observed that the EP-NF5 sample, containing 5 wt.% cellulose nanofibrils, exhibited the highest water absorption, approximately 2.25%. This high value suggests that at higher loadings, cellulose nanofibrils may agglomerate or introduce porosity within the matrix, compromising the barrier properties of the coating. This was followed by EP-NF2.5, which has a water absorption of around 1.95%. A similar observation was made in a study of the water absorption behaviour of recycled cellulose fibres reinforced epoxy composites by Sekar et al. (2022). They observed that an addition of cellulose to epoxy composites led to an increase in water absorption properties. These imply that cellulose's hydrophilic nature may contribute to increased water uptake if not well-dispersed. The chemical reason for this is due to the presence of hydroxyl groups in the cellulose structure, which attract water molecules and bind with them through hydrogen bonding (Etale et al., 2023).

The plain epoxy coating (EP) absorbed about 1.85%. In contrast, coatings incorporated with nanoclay demonstrated improved resistance to water. For instance, EP-C5 exhibited the lowest water absorption value of about 1.45%, and EP-C2.5 showed a slightly higher absorption of 1.65%. The low water uptake by these samples could be attributed to the nature of nanoclay, to creates a better tortuous path for water molecules and enhances barrier properties (Muralishwara et al., 2022). A similar observation has been made by Muralishwara et al. (2022) in their study of the effect of nanoclay on the water absorption properties of recycled cellulose fiber reinforced epoxy hybrid composites. Their result showed that the maximum water uptake of RCF/epoxy decreased significantly by about 34% when 5 wt.% Nanoclay was added. Hybrid coatings containing both CNF and nanoclay showed intermediate performance. EP-C2.5NF2.5 and EP-C5NF2.5 recorded water absorption values of 1.75% and 1.60%, respectively, indicating that the combined effect of the two fillers improved moisture resistance relative to CNF-only systems but did not surpass the nanoclay-only formulations. These findings suggest that the use of nanoclay alone provides better resistance to water absorption, likely due to its layered structure. The synergistic effect observed in cellulose nanofibrils-nanoclay hybrid systems further underscores the importance of optimizing filler combinations and ratios.

Investigating the water absorption behavior of nanocomposite coatings in saline environments is critical for evaluating their potential application in marine or coastal settings. Figure 5 presents the percentage of water absorbed by various epoxy-based coatings after exposure to a saltwater environment. From the figure, all samples exhibited lower water absorption in saline water compared to their performance in fresh water, as previously presented in Figure 4. This reduction can be attributed to the higher ionic strength and density of saline water, which reduces the mobility and diffusivity of water molecules into the polymer matrix, thereby limiting overall water uptake. The plain epoxy (EP) coating showed a water absorption value of about 1.54% in saltwater, compared to 1.85% in freshwater. The EP-NF5 sample recorded the highest absorption in the saline environment at 1.85%, although still lower than its freshwater value of 2.25%. This suggests that cellulose nanofibrils, being hydrophilic, can still absorb moisture in marine conditions. The EP-C5 coating showed the lowest water absorption in saline conditions at approximately 1.2%, compared to 1.45% in freshwater. This confirms that nanoclay still maintains its tortuous pathway even in harsh environments.

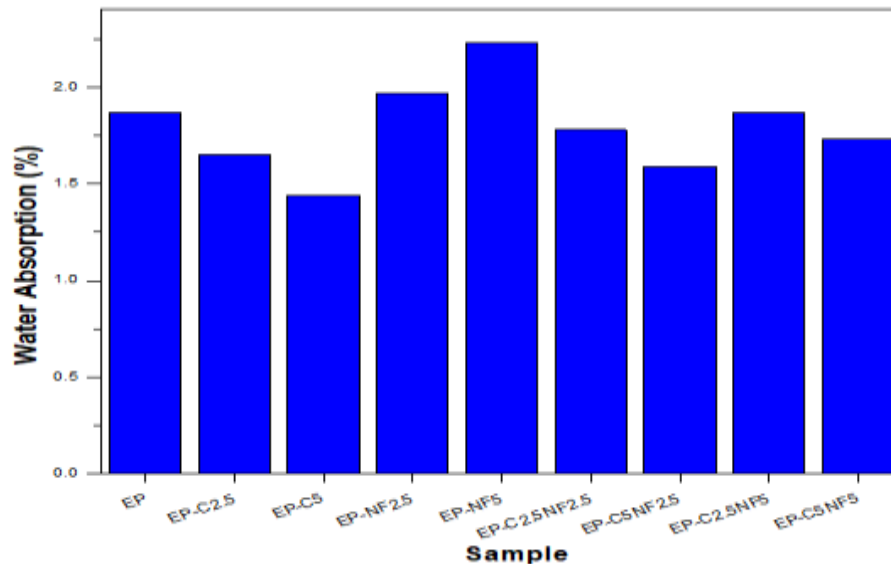


Figure 4: Water absorption rate of the nanocomposite coatings

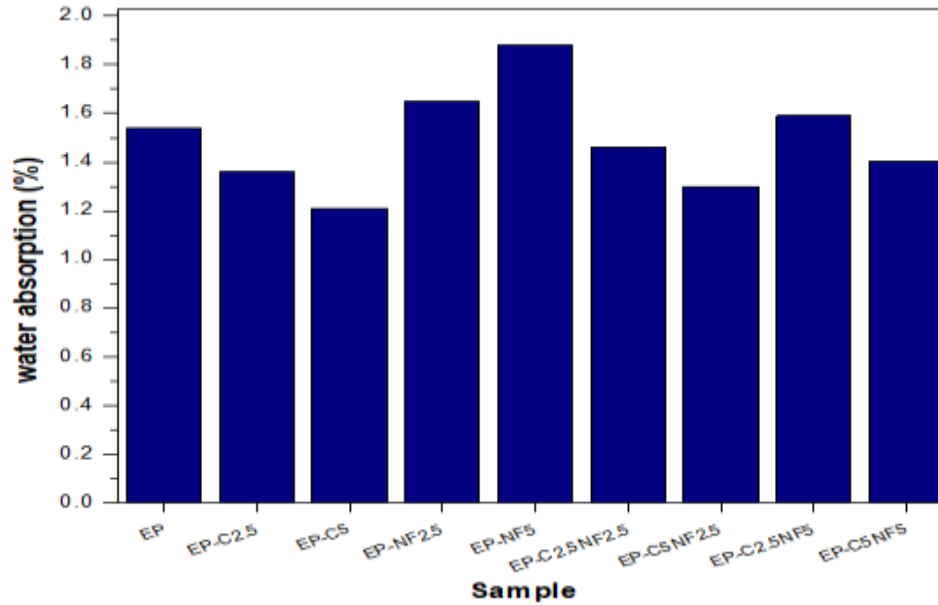


Figure 5: Saline absorption rate of the nanocomposite coatings

3.4 Immersion Test Result

The coated steel substrates were submerged in a 3.5 wt.% NaCl solution for 7 days. As seen from Fig. 6 (a) and (b), incorporating cellulose fibrils/clay nanocomposites enhanced the steel surface's resistance to corrosion. Although there was less corrosion in the epoxy/NC/CNF-coated steel substrate had traces of blisters in some places on the structured surface Fig. 6 (d)), presumably, an outcome of water leaking through the coating. This could be explained by CNF's hydrophilic properties, which raise the likelihood of water absorption.

As illustrated in Figure 5, the neat EP and EP-NF5 incurred the most weight loss due to corrosion compared to the impacted coatings. Additionally, out of all the coated samples, the steel substrate coated with EP-C5NF2.5 exhibited the best anticorrosion behavior (the least amount of weight loss).

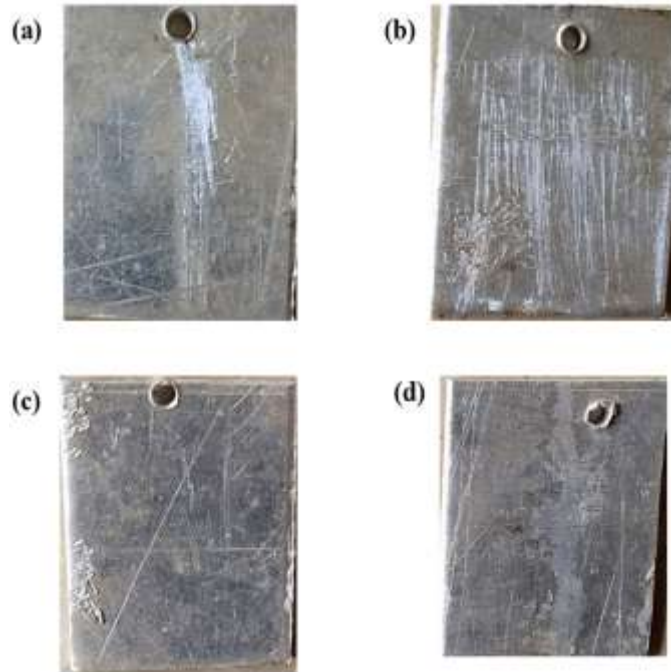


Figure 6: Photographic image of uncoated steel samples

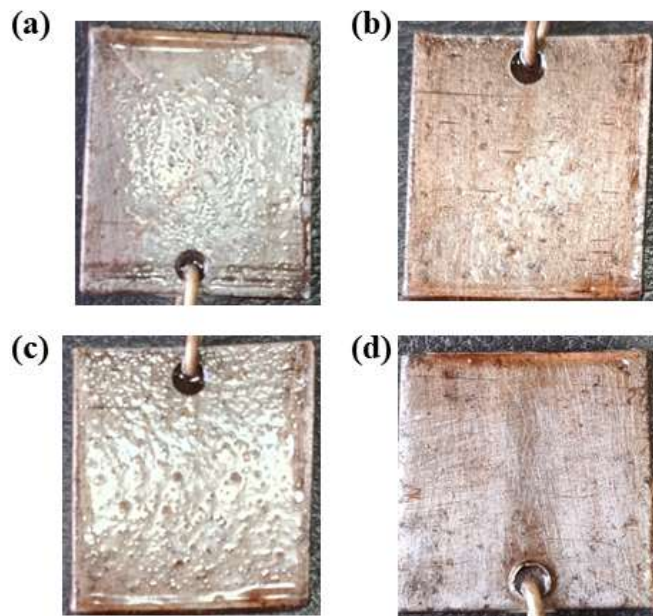


Figure 7: Steel substrates coated with (a) epoxy/NC, (b) epoxy/CNF/NC, (c) plain epoxy, and (d) epoxy/CNF after curing.

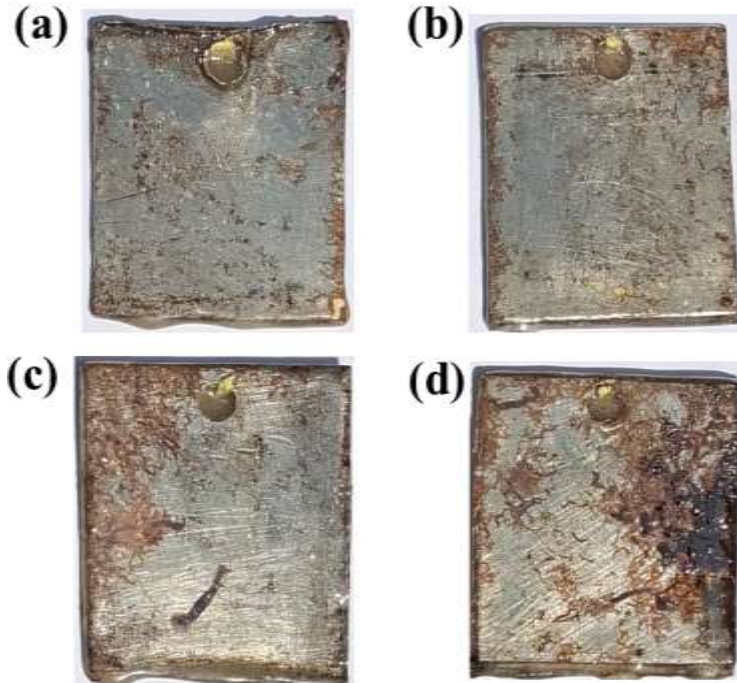


Figure 8: Steel substrates coated with (a) epoxy/NC, (b) epoxy/CNF/NC, (c) plain epoxy, and (d) epoxy/CNF immersed in 3.5 wt. % NaCl solution for 7 days

4.0. Conclusion

This study explored the development and evaluation of epoxy-based nanocomposite coatings reinforced with encapsulated cellulose nanofibrils (CNF) and nanoclay (NC) for enhanced water resistance and anticorrosion applications. The research successfully demonstrated the potential of using interfacial polymerization to encapsulate nanofillers and incorporate them into epoxy matrices, addressing the inherent limitations of conventional epoxy coatings in moisture-rich or marine environments. Characterization techniques such as FTIR and TEM confirmed the successful synthesis and dispersion of nanofillers, with an observed nanoclay particle size of 7–15 nm. The water absorption tests under both freshwater and saline conditions showed a marked improvement in barrier properties upon the incorporation of nanoclay and CNF. Notably, coatings reinforced with 5 wt.% nanoclay (EP-C5) and hybrid nanocomposites containing 5 wt.% NC and 2.5 wt.% CNF (EP-C5NF2.5) exhibited the lowest water absorption. This result highlights the synergistic benefit of combining nanoclay and CNF, effectively forming a tortuous diffusion path for water molecules.

This study demonstrated that encapsulated CNF and NC nanocomposites can significantly enhance the performance of epoxy coatings in corrosive environments. It establishes a foundation for sustainable and effective corrosion-resistant technologies, contributing to longer service life and reduced maintenance of metal structures. The findings have practical implications for designing sustainable, high-performance protective coatings for marine, construction, and industrial infrastructure. Also, based on the outcomes of this study, it is recommended that future research explore long-term aging behaviors and mechanical property retention under cyclic salt spray and UV conditions to validate durability. Additionally, the scalability of the encapsulation process for industrial coating production should be investigated.

Acknowledgements

The authors are grateful for the support from the management and staff of the Polymer Engineering Laboratory, Faculty of Engineering, Nnamdi Azikwe University, Awka.

References

- Arukalam, I. O., Timothy, U. J., Madu, I. O., & Achor, J. O. 2021. Improving the water barrier and anticorrosion performances of epoxy-chitosan coatings via silane modification. *Journal of Bio-and Tribo-Corrosion*, 7, 1-13.
- Dhanola, A., Bisht, A. S., Kumar, A., & Kumar, A. 2018. Influence of natural fillers on physico-mechanical properties of luffa cylindrica/polyester composites. *Materials Today: Proceedings*, 5(9), 17021-17029.
- Ewulonu, C. M., Chukwunke, J. L., Nwuzor, I. C., & Achebe, C. H. 2020. Fabrication of cellulose nanofiber/polypyrrole/polyvinylpyrrolidone aerogels with box-Behnken design for optimal electrical conductivity. *Carbohydrate Polymers*, 235, 116028.
- Ghazi, A., Ghasemi, E., Mahdavian, M., Ramezanzadeh, B., & Rostami, M. 2015. The application of benzimidazole and zinc cations intercalated sodium montmorillonite as smart ion exchange inhibiting pigments in the epoxy ester coating. *Corrosion Science*, 94, 207-217.
- Gite, V. V., Tatiya, P. D., Marathe, R. J., Mahulikar, P. P., & Hundiware, D. G. 2015. Microencapsulation of quinoline as a corrosion inhibitor in polyurea microcapsules for application in anticorrosive PU coatings. *Progress in Organic Coatings*, 83, 11-18.
- Habib, S., Hassanein, A., Kahraman, R., Ahmed, E. M., & Shakoor, R. 2021. Self-healing behavior of epoxy-based double-layer nanocomposite coatings modified with Zirconia nanoparticles. *Materials & Design*, 207, 109839.
- Iheoma, C. C., & Isaac, O. I. 2016. Extender Properties of Some Nigerian Clays. *Journal of Minerals and Materials Characterization and Engineering*, 4(05), 279-291.
- Kumar, A., & Thakur, A. 2024. *Encapsulated Corrosion Inhibitors for Eco-Benign Smart Coatings*. CRC Press.
- Li, Z., Yu, Q., Zhang, C., Liu, Y., Liang, J., Wang, D., & Zhou, F. 2019. Synergistic effect of hydrophobic film and porous MAO membrane containing alkynol inhibitor for enhanced corrosion resistance of magnesium alloy. *Surface and Coatings Technology*, 357, 515-525.
- Manickam, M., Sivakumar, D., Thirumalairaj, B., & Jaganathan, M. 2016. Corrosion Inhibition of Mild Steel in 1 mol L⁻¹ HCl Using Gum Exudates of *Azadirachta indica*. *Advances in Physical Chemistry*.
- Matykiewicz, D. 2020. Hybrid epoxy composites with both powder and fiber filler: a review of mechanical and thermomechanical properties. *Materials*, 13(8), 1802.
- Mi, X., Liang, N., Xu, H., Wu, J., Jiang, Y., Nie, B., & Zhang, D. 2022. Toughness and its mechanisms in epoxy resins. *Progress in Materials Science*, 130, 100977.
- Montemor, M. 2016. Hybrid nanocontainer-based smart self-healing composite coatings for the protection of metallic assets. In *Smart Composite Coatings and Membranes* (pp. 183-209). Elsevier.
- Motlatle, A. M., Ray, S. S., & Scriba, M. 2018. Polyaniline-clay composite-containing epoxy coating with enhanced corrosion protection and mechanical properties. *Synthetic Metals*, 245, 102-110.
- Nair, S. S., Kuo, P.-Y., Chen, H., & Yan, N. 2017. Investigating the effect of lignin on the mechanical, thermal, and barrier properties of cellulose nanofibril reinforced epoxy composite. *Industrial Crops and Products*, 100, 208-217.
- Nazari, M. H., & Shi, X. 2016. Polymer-based nanocomposite coatings for anticorrosion applications. *Industrial Applications for Intelligent Polymers and Coatings*, 373-398.
- Njoku, C. N., Arukalam, I. O., Bai, W., & Li, Y. 2018. Optimizing maleic anhydride microcapsules size for use in self-healing epoxy-based coatings for corrosion protection of aluminum alloy. *Materials and Corrosion*, 69(9), 1257-1267.
- Olajire, A. A. 2018. Recent advances on organic coating system technologies for corrosion protection of offshore metallic structures. *Journal of Molecular Liquids*, 269, 572-606.
- Pathak, R., Punetha, M., Bhatt, S., Pillai, S. A., Dhapola, P. S., & Punetha, V. D. 2024. Organic and inorganic nanofillers for polymer nanocomposites: Trends, opportunities, and challenges. *Advances in Functionalized Polymer Nanocomposites*, 1-34.
- Ramesan, M., & Surya, K. 2016. Studies on electrical, thermal and corrosion behaviour of cashew tree gum grafted poly (acrylamide). *Polymers from Renewable Resources*, 7(3), 81-99.
- Sun, Y., Liu, Y., Gong, J., Han, X., Xi, Z., Zhang, J., Wang, Q., & Xie, H. 2022. Thermal and bonding properties of epoxy asphalt bond coats. *Journal of thermal analysis and calorimetry*, 1-13.
- Surendran, A., Pioteck, J., Malanin, M., Vogel, R., Kalarikkal, N., & Thomas, S. 2021. Miscibility, microstructure, and in situ cure analysis of epoxy-SAN-cloisite 20A nanocomposites. *New Journal of Chemistry*, 45(3), 1395-1403.

- Velásquez-Cock, J., Gañán, P., Posada, P., Castro, C., Serpa, A., Putaux, J.-L., & Zuluaga, R. 2016. Influence of combined mechanical treatments on the morphology and structure of cellulose nanofibrils: Thermal and mechanical properties of the resulting films. *Industrial Crops and Products*, 85, 1-10.
- Wu, J., Li, C., Hailatihan, B., Mi, L., Baheti, Y., & Yan, Y. 2022. Effect of the addition of thermoplastic resin and composite on mechanical and thermal properties of epoxy resin. *Polymers*, 14(6), 1087.
- Xu, Y., Yan, X., Zheng, H., Li, J., Wu, X., Xu, J., Zhen, Z., & Du, C. 2024. The application of encapsulation technology in the food Industry: Classifications, recent Advances, and perspectives. *Food Chemistry: X*, 101240.
- Yang, W., Feng, W., Liao, Z., Yang, Y., Miao, G., Yu, B., & Pei, X. 2021. Protection of mild steel with molecular engineered epoxy nanocomposite coatings containing corrosion inhibitor functionalized nanoparticles. *Surface and Coatings Technology*, 406, 126639.
- Zhang, Q., Xu, Y.-h., & Wen, Z.-g. 2017. Influence of water-borne epoxy resin content on performance of waterborne epoxy resin compound SBR modified emulsified asphalt for tack coat. *Construction and Building Materials*, 153, 774-782.